

Critical behavior of a model for catalyzed autoamplification

Martin Tchernookov, Aryeh Warmflash, and Aaron R. Dinner^{a)}
James Franck Institute, The University of Chicago, Chicago, Illinois 60637, USA

(Received 29 November 2008; accepted 27 February 2009; published online 2 April 2009)

We examine the critical behavior of a model of catalyzed autoamplification inspired by a common motif in genetic networks. Similar to models in the directed percolation (DP) universality class, a phase transition between an absorbing state with no copies of the autoamplifying species A and an active state with a finite amount of A occurs at the point at which production and removal of A are balanced. A suitable coordinate transformation shows that this model corresponds to one with three fields, one of which relaxes exponentially, one of which displays critical behavior, and one of which has purely diffusive dynamics but exerts an influence on the critical field. Using stochastic simulations that account for discrete molecular copy numbers in one, two, and three dimensions, we show that this model has exponents that are distinct from previously studied reaction-diffusion systems, including the few with more than one field (unidirectionally coupled DP processes and the diffusive epidemic process). Thus the requirement of a catalyst changes the fundamental physics of autoamplification. Estimates for the exponents of the diffusive epidemic process in two dimensions are also presented. © 2009 American Institute of Physics. [DOI: 10.1063/1.3101649]

I. INTRODUCTION

Many systems far from equilibrium can be described by reaction-diffusion models. Examples include molecular species in a chemostat,¹ morphogen gradients during the development of multicellular organisms,² neural systems,³ ecological niches,⁴ populations experiencing epidemics,⁵ and financial markets.⁶ Many such models exhibit a phase transition between an absorbing (or inactive) and a nonabsorbing (or active) state. Analytical and numerical treatments that account for stochastic fluctuations in such models indicate that many belong to only a handful of classes, for each of which the members conform to a set of universal scaling relations.^{7–11} The most well-studied of such class is that directed percolation (DP).^{11–15}

Here, we consider a model of catalyzed autoamplification. In the model, a molecule A binds the catalyst D to form a bound complex B that can either dissociate or create another copy of A; molecules of A are destroyed at a constant rate. Schematically,



where f , g , h , and k are the rate constants for the indicated reactions and $A \rightarrow \emptyset$ represents the loss of one copy of A. One specific realization of this general scheme is a common element of genetic circuits, a self-regulating gene. Namely, a transcription factor (A) binds to the regulatory region of its own gene (D for DNA) to activate further expression.

Qualitatively, as the net rate of producing the self-amplifying factor exceeds that of removing it, the system

undergoes a phase transition, which is superficially similar to that described above for models in the DP universality class. While single-field models of this nature have been exhaustively categorized (indeed, see Elgart and Kamenev¹⁶), the physics of systems with multiple coupled fields is much more poorly understood. To the best of our knowledge, the only previously studied models of the latter nature are successive DP processes¹⁷ and the diffusive epidemic process.^{5,18,19} Here, we exploit recent advances in simulating the quasistationary state²⁰ to show in one, two, and three dimensions that the explicit treatment of the catalyst (or gene) makes the physics of this model fundamentally different. In the process, we explore numerical issues and obtain for the first time estimates for the exponents of the diffusive epidemic process in two dimensions. The relation of the model to others studied previously is discussed.

II. MEAN-FIELD BEHAVIOR

Here, we use a mean-field treatment to introduce the critical exponents used to describe the model. For mathematical simplicity, we take all the species to have the same diffusion constant, D_0 , such that the macroscopic reaction-diffusion equations are

$$\frac{\partial C_A}{\partial t} = D_0 \nabla^2 C_A - h C_A C_D + (f + g) C_B - k C_A \quad (2)$$

$$\frac{\partial C_D}{\partial t} = D_0 \nabla^2 C_D - h C_A C_D + f C_B \quad (3)$$

$$\frac{\partial C_B}{\partial t} = D_0 \nabla^2 C_B + h C_A C_D - f C_B. \quad (4)$$

An important feature of these equations is that they conserve the catalyst, $\rho \equiv C_D + C_B = \text{constant}$.

^{a)}Electronic mail: dinner@uchicago.edu.

In the absence of fluctuations, the system is spatially homogeneous at steady state so the spatial derivative can be set to zero. The concentration of A then satisfies

$$\frac{\partial C_A}{\partial t} = -\frac{hk}{g}C_A(C_A - g\Delta\rho/k) = 0, \quad (5)$$

where $\Delta\rho = \rho - fk/gh$. Equation (5) has two solutions: $C_A = 0$ and $g\Delta\rho/k$. The former is stable for $\Delta\rho < 0$, and the latter is stable for $\Delta\rho > 0$. Thus $\Delta\rho = 0$ represents a continuous phase transition.

We characterize the system by a series of scaling laws. That for how the order parameter C_A varies with deviations from the critical density is

$$C_A \sim \Delta\rho^\beta. \quad (6)$$

From the discussion above, we immediately see that $C_A \sim \Delta\rho$ in the mean-field and thus $\beta = 1$ for $\Delta\rho > 0$.

At criticality, we expect the average order parameter to decay to zero as

$$C_A \sim t^{-\alpha}. \quad (7)$$

To find this exponent, we again consider the homogeneous system and impose the conservation law $C_D + C_B = \rho$. Then the system of equations can be written

$$\dot{\mathbf{x}} = \mathbf{J}\mathbf{x} + \mathbf{L}(\mathbf{x}), \quad (8)$$

where $\mathbf{x} = (C_A, C_B)$, \mathbf{L} is a vector containing the nonlinear terms, and J is the Jacobian of the system,

$$\mathbf{J} = \begin{pmatrix} -k - \frac{fk}{g} & g + f \\ \frac{fk}{g} & -f \end{pmatrix}. \quad (9)$$

Diagonalizing the Jacobian we find

$$\dot{\mathbf{x}}' = \mathbf{M}\mathbf{x}' + \mathbf{L}'(\mathbf{x}'), \quad (10)$$

where $\mathbf{x}' = \mathbf{U}_c^{-1}\mathbf{x}$, \mathbf{L}' is the function \mathbf{L} transformed to the new variables, \mathbf{U}_c is the matrix of eigenvectors of \mathbf{J} , and \mathbf{M} is a diagonal matrix with entries equal to the eigenvalues of \mathbf{J} ,

$$\mathbf{M} = \begin{pmatrix} 0 & 0 \\ 0 & -f - k - \frac{fk}{g} \end{pmatrix} \quad (11)$$

$$\mathbf{U}_c = \begin{pmatrix} \frac{g}{k} & -\frac{g+f}{f} \\ 1 & 1 \end{pmatrix}. \quad (12)$$

We are interested in the decay of the component of $\mathbf{x}' \equiv (x'_1, x'_2)$, which corresponds to the zero mode of the Jacobian. Explicitly,

$$\dot{x}'_1 = fC_A + (f+g)C_B. \quad (13)$$

Since $M_{22} < 0$, we do not need to consider x'_2 but can set it to zero in the long time limit. Because x'_1 corresponds to the zero mode of the Jacobian, its equation of motion has no linear terms at criticality. Examining the higher order terms contained in \mathbf{L}' reveals that the lowest order term governing

the relaxation of x'_1 is the quadratic term. In other words, we find that as $t \rightarrow \infty$, $\dot{x}'_1 \sim x'^2_1$, which implies $\alpha = 1$.

At criticality, we expect the correlation length (ξ_\perp) and time (ξ_\parallel) to become infinite, and the exponents ν_\perp and ν_\parallel are defined by

$$\xi_\perp \sim |\Delta\rho|^{-\nu_\perp} \quad (14)$$

$$\xi_\parallel \sim |\Delta\rho|^{-\nu_\parallel}. \quad (15)$$

In order to determine ν_\parallel and ν_\perp , we utilize the following analysis. Since the concentrations decay to zero, the long-time behavior of the system in the inactive regime is governed by the terms of the rate equations that are linear in the concentrations. This linear term is zero exactly at criticality, but has the coefficient $\Delta\rho$ slightly away from criticality. Thus, the equation that determines the evolution of the critical mode of the system, x'_1 , close to criticality is given by

$$\frac{\partial x'_1}{\partial t} = D_0 \nabla^2 x'_1 - (\Delta\rho)x'_1. \quad (16)$$

Since the correlation functions are only functions of differences between the two points considered, the solution to this equation for the concentration of x'_1 with initial condition $x'_1(\mathbf{x}, 0) = \delta(\mathbf{x})$ will give the correlation function $G(\mathbf{x}, t) = \langle x'_1(\mathbf{x}, t)x'_1(0, 0) \rangle$. The fundamental solution to this differential equation is easily obtained by Fourier transforming to momentum-frequency space (we distinguish functions and their Fourier transforms by their arguments),

$$G(\omega, \mathbf{p}) = \int d\mathbf{x} dt G(\mathbf{x}, t) e^{-i\omega t} e^{-i\mathbf{x} \cdot \mathbf{p}}. \quad (17)$$

We then find

$$G(\omega, \mathbf{p}) = \frac{1}{-i\omega + D_0 p^2 + \Delta\rho}. \quad (18)$$

Going back to momentum-time coordinates, we have

$$G(t, \mathbf{p}) = \int \frac{d\omega}{2\pi} \frac{e^{-i\omega t}}{-i\omega + D_0 p^2 + \Delta\rho} = e^{-(D_0 p^2 + \Delta\rho)t} \Theta(t), \quad (19)$$

where the integral was evaluated by closing the upper half-plane if $t < 0$ and the lower half-plane if $t > 0$. To come back to spatial coordinates, we need to evaluate the following:

$$\begin{aligned} G(t, \mathbf{x}) &= \int \frac{d^d p}{(2\pi)^d} e^{-i\mathbf{p} \cdot \mathbf{x}} e^{-(D_0 p^2 + \Delta\rho)t} \\ &= \int \frac{d^d p}{(2\pi)^d} e^{-iD(\mathbf{p} + i\mathbf{x}/2D_0 t)^2} e^{-x^2/4D_0 t - \Delta\rho t} \\ &\sim e^{-x^2/4D_0 t - \Delta\rho t}. \end{aligned} \quad (20)$$

From here, we see that $G(t, 0) \sim e^{-t/(1/\Delta\rho)}$, and so $\nu_\parallel = 1$. To extract the dependence of the spatial correlation length on the distance from criticality without considering time-dependent effects, we set $(\Delta\rho)t = K$ where K is a constant. Then,

$$G(t, \mathbf{x}) \sim e^{-x^2/(4D_0K/\Delta\rho)}, \quad (21)$$

which gives us $\nu_{\perp}=1/2$. In summary, the mean-field critical exponents are $\beta=1$, $\nu_{\perp}=1/2$, $\nu_{\parallel}=1$, and $\alpha=1$, which are identical to the mean-field values for DP.

III. NUMERICAL RESULTS

Below a critical dimension, fluctuations that are correlated in time and space can profoundly influence the collective behaviors of interest in such models, and it is important to go beyond the mean field in analysis. Unfortunately, exact and even approximate (renormalization group) methods that account for stochastic effects can be challenging to apply to all but the simplest such models. Although the total amount of catalyst is conserved, the numbers of A, B, and D molecules can all vary at any given point in space. While a field theoretic treatment of a reduced model is possible (M.T., A.W., and A.R.D., in preparation), here we focus on a numerical treatment of the full model. To this end, we first describe the algorithm used in the simulations and then present the results for the critical exponents.

A. Algorithm

All simulations were performed using a spatially explicit version of the Gillespie algorithm²¹ in which reactions at different sites were considered independent and diffusion was modeled by hopping reactions between sites. At each lattice site, a total of seven reactions were possible, the four reactions which define the model of autoamplification [Eq. (1)], and three different diffusion reactions, one for each species. We label the reactions by the index j and the lattice site by the index x . The propensity for each reaction to occur on lattice site x is $a_j^{(x)}=k_jR_j^{(x)}$ where k_j is the rate constant for reaction j and $R_j^{(x)}$ is the total number of combinations of reactant species on site x . For example, for the reaction $A+D \rightarrow B$, $R_j^{(x)}=n_A^{(x)}n_D^{(x)}$. In each step, first a lattice site was chosen with the probability of choosing each lattice site proportional to the total propensity for a reaction to occur at that site $a_{\text{tot}}^{(x)}=\sum_j a_j^{(x)}$. Then, a reaction was chosen from among the seven possible reactions at that site, with the probability of choosing reaction j proportional to $a_j^{(x)}$. If a diffusion reaction was chosen, a molecule was moved to a nearest neighbor of the current lattice site chosen at random. We used periodic boundary conditions and did not impose any limit on the number of particles, which could occupy a given site. After each reaction, the simulation time was advanced according to $\Delta t = -(1/a_{\text{tot}})\log r_1$ where $a_{\text{tot}}=\sum_x a_{\text{tot}}^{(x)}$ and r_1 is a random number chosen from a uniform distribution on the interval $0 < r_1 \leq 1$.

For our model on a finite lattice, the system must eventually access the absorbing state, so that in the stationary state the system has zero copies of A with probability one. Instead of considering the true stationary state, much more can be learned from studying the quasistationary distribution, which is the distribution conditioned on the system remaining in the active phase.²² From simulations of the quasistationary state, we calculated two quantities, the average value

of the order parameter and the average time for the system to relax to the absorbing state. If we label configurations by the index C , we define the latter quantity to be

$$t_a = \sum_C P(C) \langle t(C \rightarrow 0) \rangle, \quad (22)$$

where $P(C)$ is the probability of observing configuration C in the quasistationary state, 0 labels the absorbing state, and the average is taken over many trajectories, which begin at configuration C . At the critical point, the average density of A particles and average time for the system to relax to the absorbing state are expected to obey the power law relations¹⁹

$$t_a \sim L^z \text{ and } \langle A \rangle \sim L^{\beta/\nu_{\perp}}. \quad (23)$$

The critical exponent z relates the spatial and temporal scaling properties of the system and is given in terms of the critical exponents discussed in Sec. II by $z = \nu_{\parallel}/\nu_{\perp}$.

To determine $\langle A \rangle$ and t_a , we ran long simulations. We began each simulation by placing one D molecule on each lattice site and a fixed number of A molecules at random locations on the lattice such that the initial density of A was 0.1 molecules per lattice site. We then utilized the spatially explicit version of the Gillespie algorithm described above to evolve the system in time until it hit the absorbing state. To reset the system from the absorbing state, we used the method of de Oliveira and Dickman,²⁰ which has been shown to sample the quasistationary distribution and to provide accurate results for the critical behavior of other reaction-diffusion models with an absorbing state.¹⁹ Namely, as the simulation was running, we maintained a list of previously visited configurations. There was a fixed probability per unit time to store a configuration to the list, so that if a state was visited for time Δt in the continuous time algorithm, it had probability $p_{\text{rep}}\Delta t$ of being added to the list where p_{rep} is a parameter fixed throughout the simulation. When the simulation accessed the absorbing state, we reset it to a randomly chosen configuration on the list. We stored a total of $N_s=1000$ configurations and set $p_{\text{rep}}=10^{-3}$ inverse time units, where one time unit is equal to the inverse of the rate of removal of A molecules (k^{-1}). We found that these values ensured that the average time on the list ($t_L=N_s/p_{\text{rep}}=10^6$ time units) was significantly longer than the average time to visit the absorbing state (t_a) so that the system retained a memory that extended further than the last visit to the absorbing state. t_L must also be chosen to be short enough to allow the list to evolve or else fluctuations in the composition of the list can cause the averages to be very slow to converge. To ensure that the same configurations were not chosen repeatedly before the list had been populated, we did not retrieve configurations from the list until it was full. If the system accessed the absorbing state before this time, we began from a new random configuration as at the beginning of the simulation. We also did not begin recording statistics for the calculations of $\langle A \rangle$ and t_a until the list was fully populated. The time to convergence varied depending on the lattice size and dimension but was typically of order 10^7 simulation time units, which corresponds to several days of central processing unit (CPU) time.

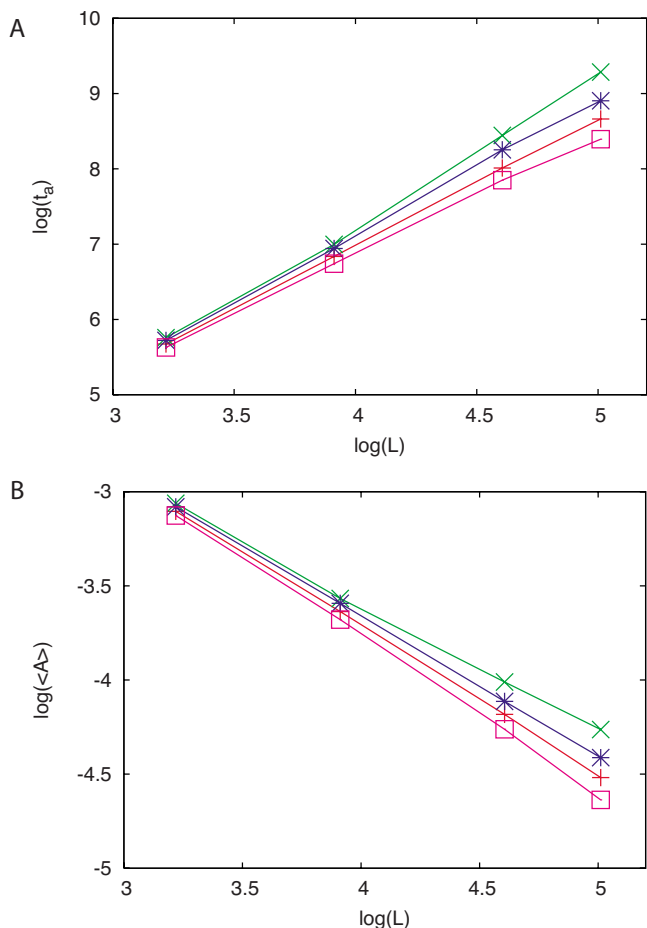


FIG. 1. (Color online) Determination of the exponents β/ν_{\perp} and z by analysis of the scaling behavior for (a) t_a and (b) $\langle A \rangle$. Results shown are for $d=2$; analogous results were obtained in $d=3$. Similar results were obtained in $d=1$ except that scaling behavior was observed for a wider range of values of g . Lines correspond to $g=1.095$ (\square), $g=1.097$ ($+$), $g=1.099$ ($*$), and $g=1.101$ (\times).

B. Critical exponents

Using the procedure described above, we performed simulations in one, two, and three dimensions and calculated the values of $\langle A \rangle$ and t_a as functions of lattice size. In one dimension, we used lattice sizes of 200, 500, 1000, and 1500, in two dimensions we used 25×25 , 50×50 , 100×100 , and 150×150 , and in three dimensions we used $10 \times 10 \times 10$, $15 \times 15 \times 15$, and $20 \times 20 \times 20$. We set the values of all other parameters to one, varied the creation rate for A (g), and searched for the point where $\langle A \rangle$ and t_a showed a power law dependence on the lattice size. The results of this analysis in two dimensions are shown in Fig. 1. In two and three dimensions, we only observed scaling behavior for a small range of values of g , which allowed us to accurately determine the critical point to be at $g_c=1.098(3)$ and $g_c=1.020(2)$, respectively. In one dimension, we observed nearly linear behavior over a wider range ($g_c=1.7(1)$). Nonetheless, because the slopes of all of these lines were nearly the same, we were able to obtain an estimate for the critical exponents.

These simulations only determine the ratios of exponents β/ν_{\perp} and $z=\nu_{\parallel}/\nu_{\perp}$. To find the value of β , we ran similar simulations away from the critical point and calculated $\langle A \rangle$ in each simulation. We used the same values of L as above and

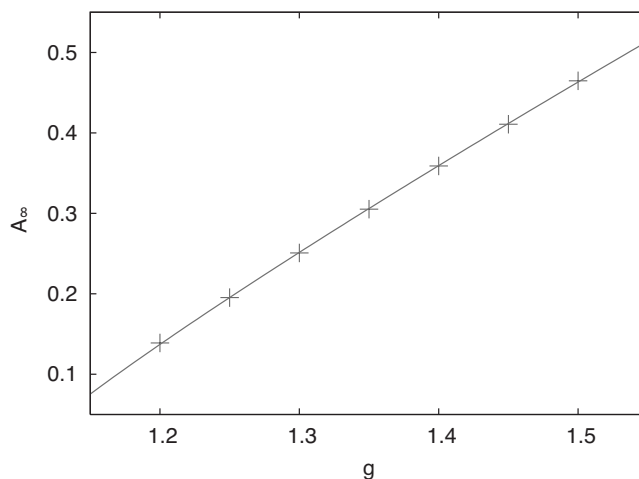


FIG. 2. Determination of the exponent β in two dimensions. Points show A_{∞} as a function g determined from simulations. The line is a fit to the function $A_{\infty}=K(g-g_c)^{\beta}$. g_c was fixed to be at 1.098 and the fit gave $\beta=0.89$ and $K=1.04$.

fit the results to the function $\langle A \rangle(L)=A_{\infty}(1-e^{-cL})$ to extrapolate to infinite lattice size. We then fit the dependence of A_{∞} on g to the function $A_{\infty}(g)=K(g-g_c)^{\beta}$ to determine the value of β . The results for two dimensions are shown in Fig. 2 and yield $\beta=0.89(2)$. A similar analysis in three dimensions showed $\beta=0.990(5)$ very close to the mean-field value. We were unable to determine the value of β in one dimension due to our inability to accurately locate the critical point.

Finally, we also directly calculated ν_{\perp} directly using the method suggested by Grassberger and Zhang.²³ This method relies on the observation that at criticality

$$\left. \frac{d \ln \langle A \rangle}{dg} \right|_{g=g_c} \sim L^{1/\nu_{\perp}}, \quad (24)$$

where the derivative is evaluated numerically as

$$\left. \frac{d \ln \langle A \rangle}{dg} \right|_{g=g_c} = \frac{1}{2h} \ln \left(\frac{\langle A \rangle(g_c+h)}{\langle A \rangle(g_c-h)} \right). \quad (25)$$

By observing the scaling behavior of this derivative, we directly determined the value of ν_{\perp} in two and three dimensions (Fig. 3). Note that this computation together with the determination of β , z , and β/ν_{\perp} above overdetermine the exponents, which provides a check on the accuracy of our computations. Directly calculating β/ν_{\perp} according to Eq. (23) gave values of 0.79(5) and 1.45(10) in two and three dimensions, respectively. Calculating these exponents separately and dividing yielded 0.77 and 1.48, so the two numerical approaches give good agreement.

As an additional check on the accuracy of our methods, we ran simulations of another model with a conserved quantity, the diffusive epidemic process (DEP), where the exact results $\nu_{\perp}=1/(2-\epsilon/2)$ for $\epsilon=4-d$ and $z=2$ in all spatial dimensions are known from theory. This process consists of

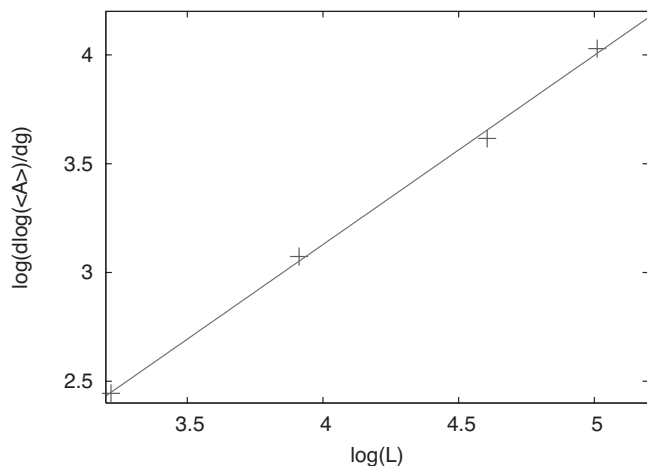


FIG. 3. Determination of the exponent ν_{\perp} in two dimensions. The line is a linear fit, which gives $\nu_{\perp}^{-1}=0.87$.

the reactions $A+B \xrightarrow{g} 2A$ and $B \xrightarrow{r} A$.^{5,18} We set $g=D_A=D_B=1$ and determined the critical point for these parameters to be at $r_c=0.5465(10)$. In two dimensions, we compute $z=1.94(10)$, which agrees with the exact result to an extent comparable to earlier calculations by Maia and Dickman¹⁹ in one dimension. Direct computation of ν_{\perp} according to Eq. (24) yielded $\nu_{\perp}=0.95(10)$. We additionally find $\beta/\nu_{\perp}=0.70(5)$ and $\beta=0.76(5)$ for $d=2$, which yields $\nu_{\perp}=1.09(11)$. Thus, both methods of calculating ν_{\perp} agree with the theoretical result $\nu_{\perp}=1$ to within simulation error. Having validated the procedure, we summarize the values for all the critical exponents determined in the catalyzed autoamplification (CA) simulations in Table I; comparisons to results for other models are provided in Tables II and III.

We also performed short simulations, which monitor the evolution of the system beginning with a single molecule at the center of the lattice as proposed by Grassberger and Delatorre,²⁴ but we found that these simulations gave values of the critical exponents in disagreement with our steady-state simulations. We attribute this to two sources of error in the short-time simulations. First, there is an ambiguity in choosing the initial configuration. In the case of a single species model,²⁴ the procedure for initializing the short time simulations is straightforward. A single particle is placed in the center of the lattice. However, in our multispecies model, the situation is more complicated. In particular, although it is clear that the simulations should begin with a single molecule of A at the center of the lattice, it is unclear how to choose the initial configuration of the B and D molecules.

TABLE I. Critical exponents for the model of catalyzed autoamplification. The number in parenthesis indicates the uncertainty on the rightmost decimal place(s). Uncertainties were calculated by determining the values of the exponents at either end of the range of values for which we observed critical behavior.

	β/ν_{\perp}	z	β	ν_{\perp}
1D	0.45(5)	1.25(5)
2D	0.79(5)	1.67(12)	0.89(2)	1.15
3D	1.45(10)	1.67(15)	0.990(5)	0.67

TABLE II. The z critical exponent for the CA, DP (Ref. 10), and DEP in one (Ref. 19) and two dimensions.

	CA	DP	DEP
1D	1.25(5)	1.580 745(10)	2.02(4)
2D	1.67(12)	1.76(3)	1.94(10)
3D	1.67(15)	1.90(1)	...

More importantly, as discussed below, our model can be seen as a DP model with disorder in the rate of creation. Such disorder is known to disrupt the universality of the short time exponents so that they become parameter dependent and break the connection between the short time and long time scaling behavior, which is present in DP.²⁵ Thus one cannot probe the steady-state behavior of the model by examining only its short-time behavior.

IV. DISCUSSION

We examined the critical behavior of a model of catalyzed autoamplification. In this model, one species (A) binds to a catalyst (D), and the bound state (B) generates additional copies of A. A key feature of the model is that the total amount of catalyst (C_B+C_D) is conserved. A phase transition is observed between an active state with finite amounts of A and B and an inactive state with only D. A mean-field analysis showed that the system can be characterized by a single order parameter, which is a linear combination of C_B and C_A . Numerical studies of the critical behavior of the discrete, stochastic model in one, two, and three dimensions established that the model exhibits scaling behavior but is not a member of previously identified universality classes.

For our numerical investigations we utilized a method for simulating the quasistationary state of a stochastic process introduced by Dickman and co-workers.^{19,20} Even with this enhanced sampling method, the results presented here required several days of CPU time for each data point, and would have been impossible to obtain with conventional simulations. Our results show that this algorithm can be usefully employed in cases where the better known method based on short-time simulations²⁴ cannot be applied. It would be interesting to compare the performance of the two methods for a model in which both are applicable.

The phase transition we examined is one which occurs between an active and an inactive phase at the point where amplification (branching) and removal (annihilation) are balanced. Most such models belong to the DP class, but some with additional or different exponents from DP have also been described. An example is the diffusive epidemic process, in which there is a conserved quantity; above, we provided the first numeric evaluation of the exponents of that model in two dimensions. Linear or quadratic coupling between DP processes also changes the critical exponents of the downstream processes.^{17,26}

It is interesting to speculate about the physics that underlie the differences between the model examined here and those in the DP class. It is possible to view the central physics of the model of CA as containing the two reactions: $A \rightarrow 2A$ and $A \rightarrow \emptyset$ just as for DP. However, in the model ex-

TABLE III. The β , ν_{\perp} , and β/ν_{\perp} critical exponents for the CA, DP (Ref. 10), and DEP in one (Ref. 19) and two (present work) dimensions.

	β			ν_{\perp}			CA	DP	DEP
	CA	DP	DEP	CA	DP	DEP			
1D	...	0.276 486(8)	0.38(5)	...	1.096 854(4)	2.0(2)	0.45(5)	0.25 207(2)	0.192(4)
2D	0.89(2)	0.584(4)	0.76	1.15	0.734(4)	0.95(10)	0.79(5)	0.795(10)	0.70(5)
3D	0.990(5)	0.81(1)	...	0.67	0.581(5)	...	1.45(10)	1.39(3)	...

amined here, the rate for the branching reaction is not a constant but instead fluctuates in each lattice site according to how much catalyst is currently present at that site. Thus, the model is similar to a DP type model in which the rate for branching fluctuates in space and time. At any given lattice site, these fluctuations in the rate do not relax exponentially but instead display a purely diffusive dynamics, which results from the fact that the total amount of catalyst is a conserved quantity whose dynamics are not influenced by the concentration of A.

Renormalization group (RG) analysis of a reduced model suggests that the background field $C_B + C_D$ becomes a static Gaussian field without any correlation between neighboring lattice sites in the limit of long times (M.T., A.W., and A.R.D., in preparation). This limit corresponds to spatially quenched disorder, which has been investigated in other contexts. Such disorder has been shown to alter the critical behavior of models²⁵ and in one case to destabilize the only RG fixed point leading to a breakdown in critical scaling.²⁷ In our model, the disorder destabilizes the DP fixed point and causes the RG flow to arrive at a different fixed point. Thus critical scaling is still observed, but the values of the critical exponents are different from DP. Spatially quenched disorder has also been shown to cause the exponents governing cluster formation starting from a single molecule to become parameter dependent,²⁸ which could explain why short-time simulation methods²⁴ did not produce accurate results for our model. It would be interesting to explore whether the effects of disorder can be captured by systematically adding background species to reaction-diffusion systems.

ACKNOWLEDGMENTS

We thank Jack Cowan for helpful discussions and a critical reading of the manuscript. This research was supported by the National Science Foundation and a Searle Scholarship to A.R.D.

- ¹F. Schlogl, *Z. Phys.* **253**, 147 (1972).
- ²H. Meinhardt, *Curr. Top. Dev. Biol.* **81**, 1 (2008).
- ³M. A. Buice and J. D. Cowan, *Phys. Rev. E* **75**, 051919 (2007).
- ⁴A. L. Lin, B. A. Mann, G. Torres-Oviedo, B. Lincoln, J. Kas, and H. L. Swinney, *Biophys. J.* **87**, 75 (2004).
- ⁵F. van Wijland, K. Oerding, and H. Hilhorst, *Physica A* **251**, 179 (1998).
- ⁶D. Becherer, *Proc. R. Soc. London, Ser. A* **460**, 27 (2004).
- ⁷B. P. Lee, Ph. D. thesis, UCSB (1994).
- ⁸B. P. Lee and J. Cardy, *J. Stat. Phys.* **80**, 971 (1995).
- ⁹J. Cardy, e-print arXiv:cond-mat/9607163.
- ¹⁰G. Odor, *Rev. Mod. Phys.* **76**, 663 (2004).
- ¹¹U. C. Täuber, M. Howard, and B. P. Vollmayr-Lee, *J. Phys. A* **38**, R79 (2005).
- ¹²J. L. Cardy and R. L. Sugar, *J. Phys. A* **13**, L423 (1980).
- ¹³H. K. Janssen, *Z. Phys. B* **42**, 151 (1981).
- ¹⁴D. Elderfield and D. D. Vvedensky, *J. Phys. A* **18**, 2591 (1985).
- ¹⁵H. K. Janssen and U. C. Täuber, *Ann. Phys.* **315**, 147 (2005).
- ¹⁶V. Elgart and A. Kamenev, *Phys. Rev. E* **74**, 041101 (2006).
- ¹⁷Y. Y. Goldschmidt, H. Hinrichsen, M. Howard, and U. C. Täuber, *Phys. Rev. E* **59**, 6381 (1999).
- ¹⁸R. Kree, B. Schaub, and B. Schmittmann, *Phys. Rev. A* **39**, 2214 (1989).
- ¹⁹D. S. Maia and R. Dickman, *J. Phys.: Condens. Matter* **19**, 065143 (2007).
- ²⁰M. M. de Oliveira and R. Dickman, *Phys. Rev. E* **71**, 016129 (2005).
- ²¹D. T. Gillespie, *J. Phys. Chem.* **81**, 2340 (1977).
- ²²R. Dickman and R. Vidigal, *J. Phys. A* **35**, 1147 (2002).
- ²³P. Grassberger and Y. Zhang, *Physica A* **224**, 169 (1996).
- ²⁴P. Grassberger and A. Delatorre, *Ann. Phys.* **122**, 373 (1979).
- ²⁵H. Hinrichsen, *Adv. Phys.* **49**, 815 (2000).
- ²⁶H. K. Janssen, e-print arXiv:cond-mat/9901188.
- ²⁷H. K. Janssen, *Phys. Rev. E* **55**, 6253 (1997).
- ²⁸I. Webman, D. Ben Avraham, A. Cohen, and S. Havlin, *Philos. Mag. B* **77**, 1401 (1998).